Supporting Information for "Variations of Low-latitude Thermospheric Winds and Temperature during the 2020/2021 Major Sudden Stratospheric Warming as Observed by ICON and GOLD Satellites"

Erdal Yiğit[1], Ayden L. S. Gann [1], Alexander S. Medvedev[2], Federico Gasperini[3], Md Nazmus Sakib[1], Qian Wu[4,5]

[1]George Mason University, Department of Physics and Astronomy, Space Weather Lab, Fairfax, VA, USA.
[2]Max Planck Institute for Solar System Research, Göttingen, Germany.
[3]Orion Space Solutions, Louisville, CO, USA
[4]High Altitude Observatory, NCAR, Boulder, CO, USA
[5]COSMIC Program UCAR/UCP, Boulder, CO, USA

Contents of this file

1. Supplementary Texts S1 to S2
2. Supplementary Figures S1, S2, S3

Corresponding author: Erdal Yiğit, eyigit@gmu.edu, May 22, 2023

Supplementary Texts

1 ICON, GOLD, Data Coverage and Choice

We use GOLD (Global-Scale Observations of the Limb and Disk) neutral temperature and ICON/MIGHTI (Ionospheric Connection Explorer/Michelson Interferometer for Global High-Resolution Thermospheric Imaging) horizontal vector wind data representative of two winters, i.e., non-SSW (December 2019 - January 2020) and SSW (December 2020 - January 2021) northern winters. ICON is operational since December 2019 and observes the low- to middle-latitude thermosphere between 10°S and 40°N (Immel et al., 2018). However, the data are available after 6 December 2019, therefore, for both winters, we use the 52-day data from 6 December to 26 January centered around 1 January 2021 (the SSW onset). ICON version 5 green line daytime horizontal winds have been binned daily from 90–200 km, including data with solar zenith angles less than 80° (i.e., $\chi < 80°$). Also, bins with less than 50 data points have been excluded, in order to avoid low statistical significance. We concentrated our analysis on the Northern Hemisphere low- to middle-latitude (0°–40°N). The associated latitude-local time coverage at $\sim$100 km is shown in Figure S1. ICON's latitude-local time coverage varies from month to month. Therefore, it would be inconsistent to compare the monthly mean fields. It is for this reason we have analyzed the altitude-time variations considering only daytime measurements. The typical uncertainties in MIGHTI green line wind measurements are 8.7–10 m s^{-1} (Englert et al., 2017).

GOLD observes the Far Ultraviolet (FUV) spectrum of Earth's atmosphere at geostationary orbit, from 0610 to 0040 Universal Time (UT) every day. Thermospheric temperatures are retrieved from the daytime disk scan measurements. The effective disk neutral temperatures (T_{disk}) are derived from the N_2 Lyman-Birge-Hopfield (LBH) emission profile at a height of approximately 150 km. The T_{disk} data product is created from spatial-spectral image cubes from the disk scans (Level 1C data). These pixels are binned 2×2 spatially, resulting in a data product that has a spatial resolution (nadir) of 250 km $\times$ 250 km, with a precision of $\pm$55 km (Eastes et al., 2020). We use version 4 of the level 2 T_{disk} data product. The longitude-latitude grids are fixed for all scans. The T_{disk} data file has flags for data quality issues at the file and pixel levels. Observations with dqi > 0 at both levels are not considered in our analysis. To increase signal-to-noise ratio (SNR), observations of $\chi > 65°$ have been removed. Random errors in the 2×2 binned data vary with SNR of the N_2 LBH emission and ranges from 20 (for high SNR) to 90 K (for low SNR). Figure S2 shows the spatiotemporal coverage for 2 representative days, 31 December 2019 and 31 December 2020. The coverage represents the good quality retained T_{disk} temperature profiles. In panels (d) and (i), an uneven latitude versus SZA (χ) distribution is seen. Higher latitudes are covered at higher χ's, which has implications for the observed temperatures. There is also less longitudinal coverage for high χ around -45 longitude, but otherwise there is even χ coverage across all longitudes. Two successive years were chosen to demonstrate the negligible amount of variability between the two years in terms of the orbital coverage.

In Figure 4 in the main text, a linear model was fitted to the data for each of the latitude bands in order to better visualize the variability. The standard deviation of the residuals were then used to generate the error bars in the plot, rather than the standard deviation of the raw temperature data. Therefore, the error bars in the plot should be interpreted as indicating the variability around the fitted linear trend, rather than the absolute variability in temperature.

2 Solar and Geomagnetic Condition during the Winters of 2019/2020 and 2020/2021

Figure S3 shows the solar and geomagnetic conditions in terms of the $F_{10.7}$ cm solar radio flux and the daily mean A_p index, respectively, during the non-SSW (Decembers 2019 - January 2020) and SSW (December 2020 - January 2021) northern winters. While the space weather conditions are overall relatively quiescent during both winters, the solar activity during the SSW winter is higher than during the non-SSW winter, since the former corresponds to the ascending phase of the solar activity, while the latter is the solar minimum. Although the magnetic activity is comparable in both years, it exhibits day-to-day variability with occasionally higher ac-

tivity during the SSW winter than the non-SSW winter. For Figure 3 we have removed 5 days in the non-SSW winter and 11 days in the SSW winter, corresponding to days with $A_p > 7$. The cyan shading marks the range of the data used for ICON and GOLD analysis (6 December - 26 January in both winters). Before 6 December 2019, ICON horizontal winds are not available and in all our analysis, we have excluded days before 6 December to be consistent in our comparison of the different winters as states in Section 1.

The source of these files is Geomagnetic Observatory Niemegk, GFZ German Research Centre for Geosciences, Potsdam, Germany. All files are available from: `ftp://ftp.gfz-potsdam.de/pub/home/obs/Kp_ap_Ap_SN_F107/` (Matzka et al., 2021).

References

Eastes, R. W., McClintock, W. E., Burns, A. G., Anderson, D. N., Andersson, L., Aryal, S., ... Woods, T. N. (2020). Initial Observations by the GOLD Mission. *Journal of Geophysical Research: Space Physics*, *125*(7), e2020JA027823. doi: 10.1029/2020JA027823

Englert, C. R., Harlander, J. M., Brown, C. M., Marr, K. D., Miller, I. J., Stump, J. E., ... Immel, T. J. (2017). Michelson Interferometer for Global High-Resolution Thermospheric Imaging (MIGHTI): Instrument Design and Calibration. *Space Sci Rev*, *212*(1), 553–584. doi: 10.1007/s11214-017-0358-4

Immel, T. J., England, S. L., Mende, S. B., Heelis, R. A., Englert, C. R., Edelstein, J., ... Sirk, M. M. (2018). The Ionospheric Connection Explorer Mission: Mission Goals and Design. *Space Sci Rev*, *214*(1), 13. doi: 10.1007/s11214-017-0449-2

Matzka, J., Stolle, C., Yamazaki, Y., Bronkalla, O., & Morschhauser, A. (2021). The geomagnetic Kp index and derived indices of geomagnetic activity. *Space Weather*.

3 Supplementary Figures

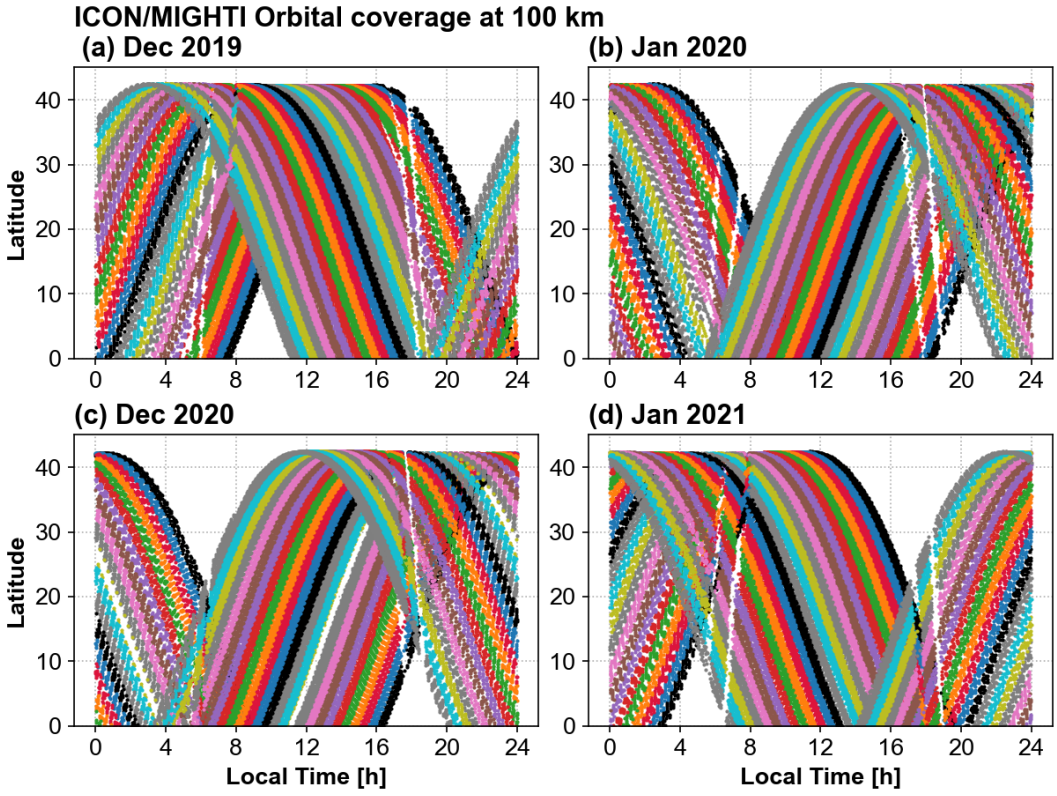

Figure S1. ICON latitude-local time coverage for the non-SSW (December 2019–January 2020) and SSW winters (December 2020–January 2021). The different colors in each panel represent a different day. White spaces show the lack of coverage.

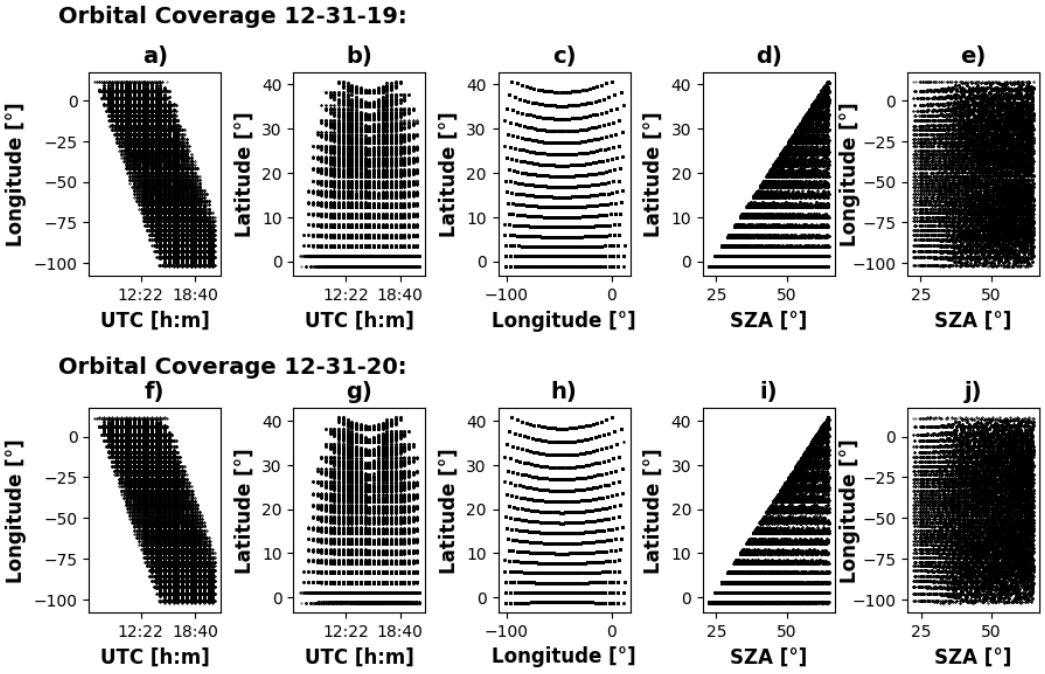

Figure S2. GOLD spatiotemporal coverage for retained T_{disk} data profiles. Panels (a)-(e) demonstrate the coverage for December 31 2019 and panels (f)-(j) demonstrate the coverage for December 31 2020.

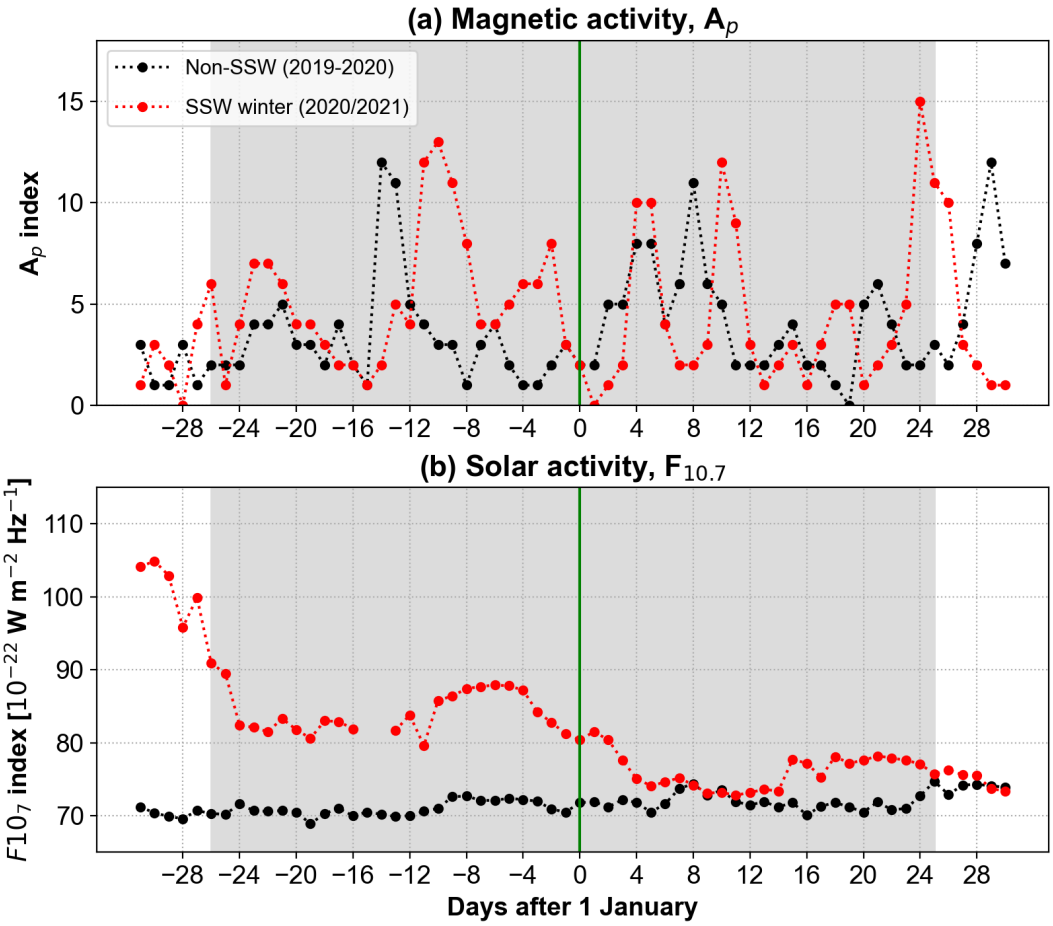

Figure S3. Variation of the (a) geomagnetic activity (A_p) and (b) solar activity ($F_{10.7}$) during the 2019/2020 non-SSW (black) and 2020/2021 SSW winters (red). Vertical green line marks the day zero, which is the onset of the major warming (i.e., 1 January 2021). The gray shading represents the time of the data analysis in this study.